# Dual-channel fiber-optic surface plasmon resonance sensor with cascaded coaxial dual-waveguide D-type structure and microsphere structure

Ling-Ling Li(李玲玲)[1], Yong Wei(魏勇)[1,†], Chun-Lan Liu(刘春兰)[1], Zhuo Ren(任卓)[1], Ai Zhou(周爱)[2], Zhi-Hai Liu(刘志海)[3], and Yu Zhang(张羽)[3]

[1] *College of Electronic & Information Engineering, Chongqing Three Gorges University, Chongqing* 404100, *China*
[2] *National Engineering Laboratory for Fiber Optic Sensing Technology, Wuhan University of Technology, Wuhan* 430070, *China*
[3] *Key Laboratory of In-fiber Integrated Optics, Ministry of Education of China, Harbin Engineering University, Harbin* 150001, *China*

(Received 8 July 2022; revised manuscript received 28 September 2022; accepted manuscript online 27 October 2022)

To address the restriction of fiber-optic surface plasmon resonance (SPR) sensors in the field of multi-sample detection, a novel dual-channel fiber-optic SPR sensor based on the cascade of coaxial dual-waveguide D-type structure and microsphere structure is proposed in this paper. The fiber sidepolishing technique converts the coaxial dual-waveguide fiber into a D-type one, and the evanescent wave in the ring core leaks, generating a D-type sensing region; the fiber optic fused ball push technology converts the coaxial dual waveguides into microspheres, and the stimulated cladding mode evanescent wave leaks, producing the microsphere sensing region. By injecting light into the coaxial dual-waveguide middle core alone, the sensor can realize single-stage sensing in the microsphere sensing area; it can also realize dual-channel sensing in the D-type sensing area and microsphere sensing area by injecting light into the ring core. The refractive index measurement ranges for the two channels are 1.333–1.365 and 1.375–1.405, respectively, with detection sensitivities of 981.56 nm/RIU and 4138 nm/RIU. The sensor combines wavelength division multiplexing and space division multiplexing technologies, presenting a novel research concept for multi-channel fiber SPR sensors.

**Keywords:** coaxial dual-waveguide, optical fiber D structure, optical fiber microsphere structure, dual-channel fiber-optic surface plasmon resonance (SPR) sensor

**PACS:** 07.07.Df, 42.81.Cn, 71.45.Gm **DOI:** 10.1088/1674-1056/ac9de3

## 1. Introduction

The optical fiber surface plasmon resonance (SPR) sensor exhibits numerous prominent features (*e.g.* compact size, excellent real-time performance, and long-distance measurement), which have been widely used in various fields in recent years.[1–3] Traditional optical fiber SPR sensors are generally based on the Kretschmann structure,[4] which uses optical fiber as the light transmission substrate, a precious metal film as the sensing film on the surface of the optical fiber, and the material to be measured outside the sensing film. The incident angle of light,[5–7] the refractive index of the substrate,[8] the type of precious metal film,[9] and the thickness of the precious metal film[10] can all be adjusted to control the dynamic range of the working wavelength of the optical fiber SPR sensor, and thus realize the multi-channel optical fiber SPR sensor of wavelength division multiplexing. Among them, Liu *et al.*[5] grounded a single-mode or few-mode fiber into a wedge shape, accomplished light incidence angle modulation by adjusting the grinding angle, and acquired a high detection sensitivity, but the sensor structure is complex, and the stability is restricted. Gold and silver have higher resonance absorption peaks among noble metals. However, silver films are quickly oxidized and require specific treatment. A few types of metal sensing membranes can be used for SPR multi-channel sensing. There is a problem with controlling the thickness of the sensing film since the sensitivity is diminished when the sensing film is thin.

The effective refractive index of the optical fiber, which serves as the Kretschmann structure's light transmission substrate, directly impact the sensing sensitivity and dynamic range of the optical fiber SPR sensor. Its effective refractive index will be influenced by both the fiber geometry and the refractive index profile, but the geometry is easier to modify. The optical fiber's geometric structure can be altered by sidepolishing,[11–13] etching,[14,15] tapering,[16,17] *etc.*, to adjust its effective refractive index. Optical fiber micromachining has high requirements for processing equipment and technical operations. Some special optical fibers have special effective refractive index, which reduces the requirements for optical fiber micromachining.

As a special optical fiber, the coaxial dual waveguide has a middle core and a ring core. Wu *et al.*[18] realized a temperature and pressure insensitive curvature sensor based on long-period fiber gratings by controlling the transmission mode of a coaxial dual-waveguide ring core. There has been no report on two fiber cores of the coaxial dual waveguide that can be used for sensing simultaneously with fiber SPR research.

[†]Corresponding author. E-mail: weiyong@hrbeu.edu.cn

© 2023 Chinese Physical Society and IOP Publishing Ltd 

Based on this, this paper proposes a novel dual-channel fiber-optic SPR sensor based on the cascade of coaxial dual-waveguide D-type and microsphere structure. This paper will make a D-type SPR sensing area utilizing side-polishing, because the outer diameter of the ring core of a coaxial dual-waveguide is 76 μm, and its evanescent field can easily leak by side-throwing; then, by melting a microsphere behind the D-type SPR sensing area, the cladding mode is excited, a sensing film is coated directly on the cladding surface behind the microsphere to construct a microsphere SPR sensing area, so as to realize the dual-channel SPR sensor based on coaxial dual-waveguide. When the light is injected into the middle core of the coaxial dual-waveguide, single-stage sensing with spherical sensor is realized, and its detection sensitivity and work waveband can be altered by adjusting the radius of microsphere. When the light is injected into the ring core of the coaxial dual-waveguide, which realizes a dual-channel sensor of D-type SPR sensing area and microsphere SPR sensing area. This paper makes the full use of the two special cores of the coaxial dual waveguide. The SPR excitation at the D-type structure is dominated by low-order modes, the microsphere structure is often excited by high-order modes, which is equivalent to adjusting the two SPR incident angle. For the SPR sensor, if the incident angle can be slightly adjusted, the adjustment of the SPR resonance operating band and sensitivity is relatively large. And for the microsphere, the SPR resonance band and sensitivity can be continuously adjusted through different microsphere diameters. D-type and microsphere structure, combined with film thickness adjustment can often achieve the two-level working band fully separated and the two-level resonance valley depth is basically the same, and the microsphere structure has a higher sensitivity. If the requirements for the separation degree of the working band, the consistency of valley depth and the sensitivity are not high, the dual-channel sensing of the double D-type structure can also be adopted.

## 2. Sensing principles and probe fabrication

### 2.1. Sensing principles

We used RSoft software to theoretically study the transmitting light field of the coaxial dual waveguide microsphere fiber. The diameter of the middle core and of the cladding are 9 μm and 125 μm, and their refractive indexes are 1.4902 and 1.485, respectively. The thickness of the ring core is 9 μm and the diameter of the microsphere is 276 μm. The simulated results are shown in Fig. 1, figure 1(a) shows the propagation path of light when passing light to the middle core, and figure 1(c) is an enlarged view of the spherical area of panel (a). Figure 1(b) shows the propagation path of light when passing light to the ring core, and figure 1(d) is an enlarged view of the spherical area of panel (b). According to the simulated results, whether to pass light to the middle core or to the ring core, the beam passes through the microsphere and causes the cladding mode to be excited, the resulting longitudinal light field distribution propagates stably. However, the excited cladding modes are different.

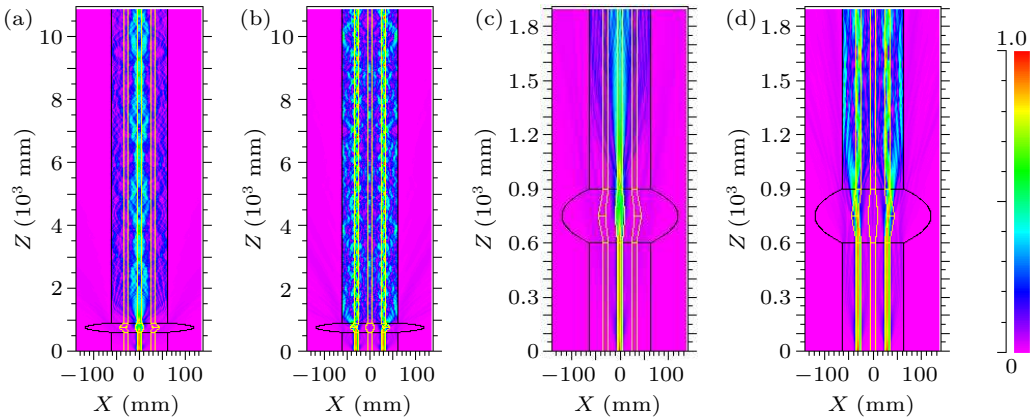



**Fig. 1.** Simulation results of (a) longitudinal light field distribution of the coaxial dual waveguide middle core with a microsphere, (b) longitudinal light field distribution of the coaxial dual waveguide ring core with a microsphere, panel (c) is an enlarged view of the spherical area of panel (a), panel (d) is an enlarged view of the spherical area of panel (b).

The coaxial dual-waveguide used in this paper has two cores: a middle core and a coaxial ring core, the diameter of the middle core is 9 μm; the ring core and the middle core have an axisymmetric distribution, with the ring core having an inner and outer diameter of 67 μm and 76 μm, respectively, and a thickness of 9 μm, which is the same as the middle core. The inner cladding is located between the middle core and the ring core, while the outer cladding, whose diameter is 125 μm, is located on the exterior of the ring core. In this paper, the ring core of the coaxial dual-waveguide is exposed to air by side-throwing, which makes the evanescent wave in the ring core contact with the gold film to form a D-type SPR sensing area; a microsphere structure is fabricated by melting on the coaxial dual-waveguide, which makes the evanescent wave

in the cladding mode excited by the microsphere expanding contact with the gold film to form a microsphere SPR sensing area. Under the operation of the microsphere, the transmitted light in the middle core readily excites the cladding mode. In the sensing area, however, the SPR phenomena created by the cladding mode and the ring core mode differ significantly. Therefore, this paper combines the cladding mode excited by the middle core of the coaxial dual-waveguide with the ring core mode together to produce an optical fiber SPR dual-channel sensor.

### 2.2. D-type sensing probe structure and fabrication

Figure 2(a) is the schematic diagram of the structure of the D-type sensing probe. The cladding in the middle section of the coaxial dual-waveguide is removed by side-polishing, the gold film coated on the exposed area of the ring core, then welded coarse core step multimode fiber on the right. The single-mode fiber faces the ring core and transmits light to the ring core. When the transmitted light reaches the side-polishing area, it leaks into the interface between the ring core and the gold film, resulting in the evanescent wave in the ring core contacts with the gold film to generate SPR effects. The coarse core step multimode fiber collects the transmitted light that generated the SPR effects and sends it to spectrometer. Finally, the spectral data are analyzed by a computer. Figure 2(b) is the end face light field diagram of coaxial dual waveguide before side-polishing when the light is injected into the ring core, and figure 2(c) is the end face light field diagram of coaxial dual waveguide after side-polishing when the light is injected into the ring core.

Figure 3 depicts the fabrication of a D-type sensing probe. We mechanically remove the coating layer of the coaxial dual-waveguide middle part and place it on the bare-fiber side-polishing equipment. We secure the two ends of the fiber with brackets and keep the fiber horizontally straight with a counterweight. We use the control box to change the horizontal reciprocal length of the scroll wheel, rotation speed, and relative placement of the scroll wheel and fiber. Abrasive paper with coarse to fine fibers is put onto the rollers in succession. The scroll wheel's speed and the polishing time can control the fiber side-polishing, and it can be observed online using a cartridge microscope and CCD, as illustrated in Fig. 3(a). The D-type fiber is put in the magnetron sputtering instrument (ETD-650MS, Vision Precision Instruments), and the nanoscale metal film is coated on the side-throwing surface, as depicted in Fig. 3(b). The right end of the coaxial dual-waveguide and the step refractive index multimode fiber with a core diameter of 105 μm (SI105/125-22/250, YOFC) are soldered by fiber optic fusion splicer to form a D-type sensing probe, the structure diagram as shown in Fig. 2(a). In this research, the residual fiber thickness after side-throwing the coaxial dual waveguide in this research is 65 μm, and the length of the side-throwing region is 2 cm, as shown in Fig. 2(c).

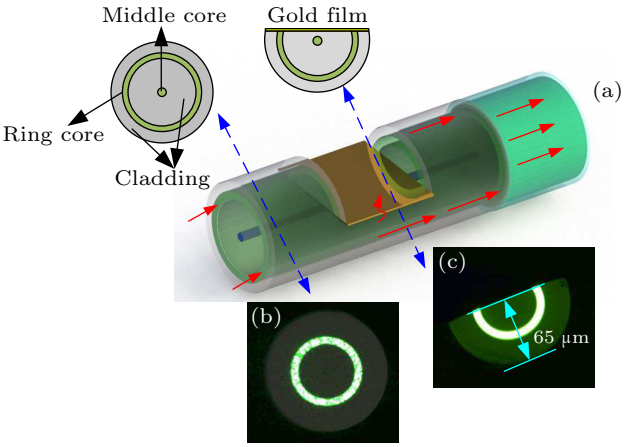



**Fig. 2.** The schematic diagram of D-type sensing probe: (a) structure diagram; (b) the end face light field diagram of coaxial dual waveguide before side-polishing when the light is injected into the ring core; (c) the end face light field diagram of coaxial dual waveguide after side-polishing when the light is injected into the ring core.

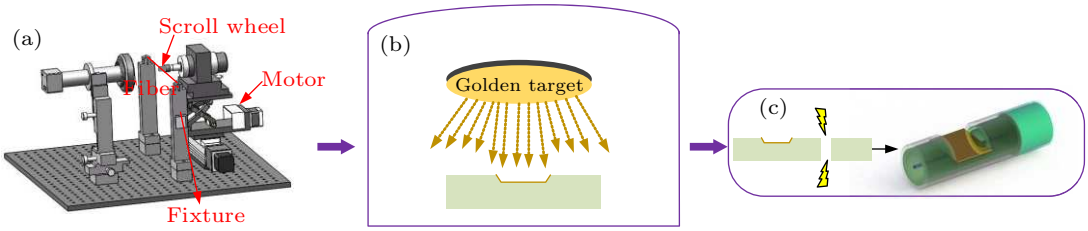



**Fig. 3.** The fabrication of a D-type sensing probe: (a) side-throwing; (b) gold film coating; (c) optical fiber splicing.

### 2.3. Microsphere sensing probe structure and fabrication

Figure 4(a) is the schematic diagram of the structure of the microsphere sensing probe. The coaxial dual-waveguide central part is electro-fused push extrusion into microspheres, to excite the cladding mode, then rotating coat nanoscale metal film on the 2 cm area behind the sphere and weld with the step refractive index multimode fiber. Light is injected into the central core of coaxial dual waveguide fiber using single-mode fiber. The radius of the coaxial dual waveguide core and cladding increases due to the microsphere structure, and when the light beam reaches the microsphere structure, the transmitted light beam in the core diffuses, the cladding mode is

excited, and the evanescent wave of transmitted light in the cladding comes into contact with the gold film, resulting in the SPR effect. The transmitted light with SPR effect is collected and supplied to the spectrometer through the large core diameter step multimode fiber, and ultimately the spectral data processing is conducted by the computer. Figure 4(b) is the micrograph of the fiber microsphere, and figure 4(c) is the end face light field diagram of coaxial dual waveguide when the light is injected into the ring core.

Figure 5 depicts the fabrication of a microsphere sensing probe. Before being placed in the fiber optic balling machine to execute discharge ball pushing, the coating layer of the coaxial dual-waveguide is mechanically removed. The fiber clamps with motor hold the two ends of the fiber, and the fiber coating stripped region is positioned in the center of the two electrodes, as indicated in Fig. 5(a). Melting time and power are set to 15 s and 65 W, respectively. When the electrode is discharged, the fiber is heated and pushed towards the center by the left and right motors to form a fiber microsphere, as illustrated in Fig. 5(b). Keep the melting time, power, and motor propulsion steady, and the microsphere diameter can be controlled by melting numbers of time. Following the completion of the ball pushing, the end-face through-light observation is done at the right 2 cm of the coaxial dual waveguide microsphere, as illustrated in Fig. 4(c), with the optical coupling in the fiber core being a high-order cladding mode. The 2-cm-long cladding coupled stable transmission zone on the right side of the microsphere is used as the sensing zone, and the right end of the coaxial dual waveguide is welded to a coarse-core step multimode fiber with a core diameter of 105 μm for light collection. A 50-nm sensing gold film is plated on the cladding of the 2-cm sensing area on the right side of the microsphere to constitute the microsphere sensing probe, as shown in Fig. 5(c).

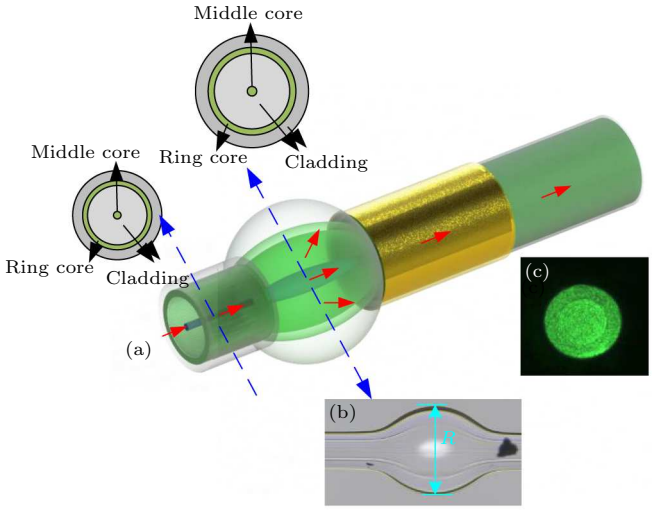



**Fig. 4.** The schematic diagram of microsphere sensing probe: (a) structure diagram, (b) the micrograph of the fiber microsphere, (c) the end face light field diagram of coaxial dual waveguide when the light is injected into the ring core.

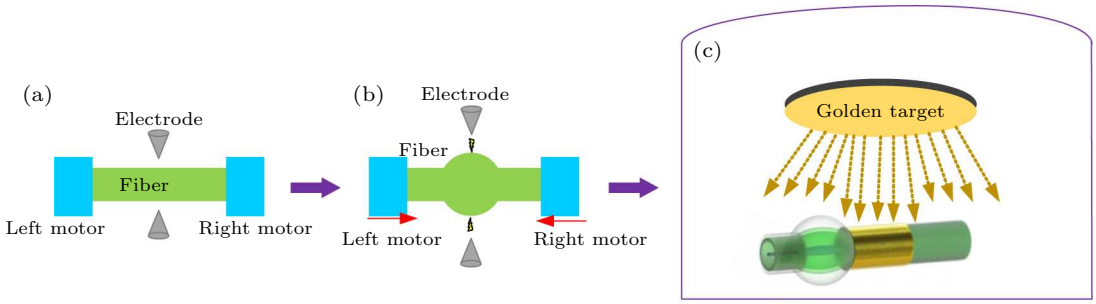



**Fig. 5.** The fabrication of a microsphere sensing probe: (a) fiber into the fiber optic balling machine, (b) discharge into balls, (c) gold film coating.

### 2.4. Experimental set-up

According to the D-type SPR sensing probe and the microsphere SPR sensing probe, constructing the refractive index sensing testing setup, as shown in Fig. 6. The fiber probe receives the light emitted by the broad-spectrum light sources (HL-2000, Ocean Optics), and the solution to be tested in the reaction cell supplies the refractive index environment. The SPR effect occurs when light transmits to the probe SPR sensing zone and the spectrum of transmitted light becomes the SPR resonance valley. The coarse-core step multimode fiber collects the light and sends the light that occurred SPR effects into the spectrometer (USB2000+, Ocean Optics), the spectrum is sent into the computer for real-time data processing. The micro-injection pumper is used to replace the different refractive index solutions in the reaction cell. As the spectral information received by the spectrometer changes, so does the position of the SPR resonance valley, allowing the refractive index of the solution to be measured in the reaction cell to be sensed by monitoring the position of the SPR resonance valley.

## 3. Experimental results and analysis

### 3.1. D-type and microsphere probes refractive index sensing testing

We build the equipment (see Fig. 6) to perform the refractive index sensing testing on the D-type and microsphere probes, respectively, and determine whether the proposed D-type and microsphere SPR sensing probes can accomplish satisfactory refractive index sensing. The microsphere diameter

of the microsphere SPR sensing probe is 233 μm; the residual fiber thickness after side-throwing the coaxial dual waveguide in this research is 65 μm, and the length of the side-throwing region is 2 cm. The sensing gold film of the two probes is 50 nm, the refractive index range of the solution to be measured is 1.333–1.405, figure 7 describes the experimental results. The SPR resonance valley shifts to a long-wavelength direction with the solution's refractive index to be measured increases. The findings displayed in Fig. 7(c) were obtained by executing a linear fit using the solution refractive index as the horizontal scales and the sensing probe's resonant wavelength as the vertical coordinate. The dynamic range of the SPR resonance valley of the D-type sensing probe is 607.05 nm–811.55 nm, the refractive index average detection sensitivity is 1563.31 nm/RIU. The dynamic range of the SPR resonance valley of the microsphere sensing probe is 593.34 nm–714.48 nm, the refractive index average detection sensitivity is 2790.31 nm/RIU. Dual-channel detection is theoretically feasible since the two sensing probes may completely separate the two resonance valleys in the spectrum without crossing over in the dynamic range when detected in high refractive index solutions.

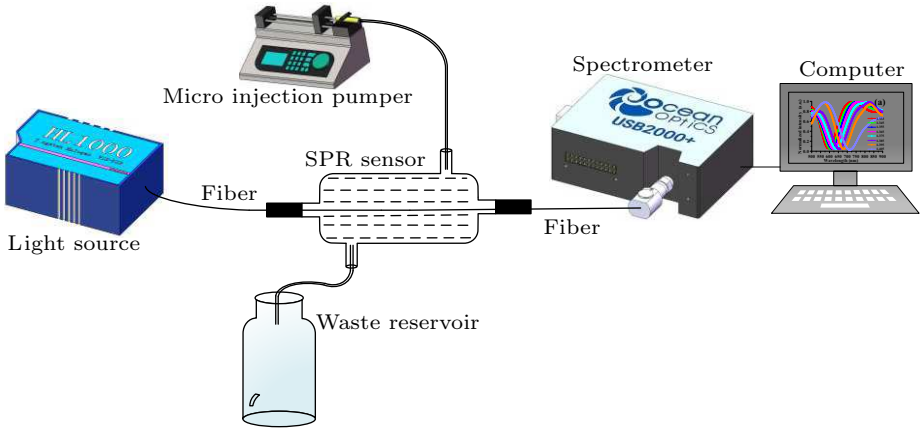



**Fig. 6.** The refractive index sensing testing setup.

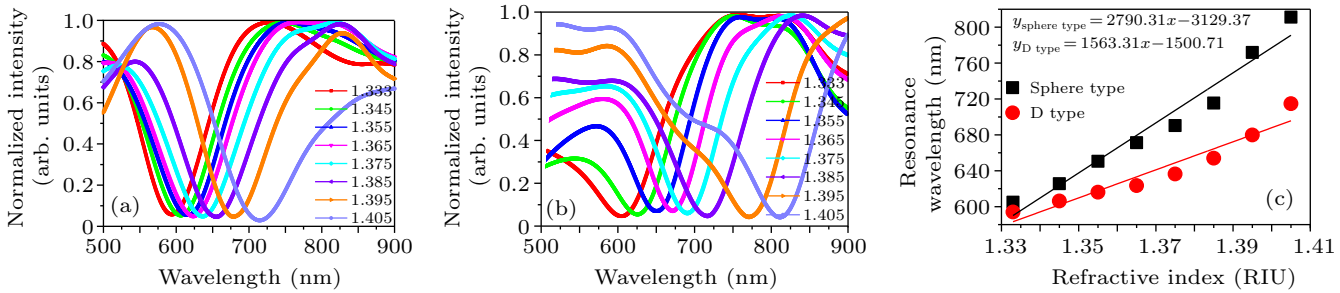



**Fig. 7.** The results of the D-type and microsphere probes refractive index sensing testing: (a) D-type sensing probe, (b) microsphere sensing probe, (c) the relationship curves of refractive index and resonance wavelength.

### 3.2. Microsphere probe microsphere diameter optimization

The dual-channel SPR sensor comprises the coaxial dual waveguide fiber D-type sensing probe and the microsphere sensing probe, as shown by the validation mentioned experiments. However, for the dual-channel SPR sensor to function, two resonance valleys must be sufficiently separated, necessitating the control of the SPR resonance bands in the two sensing regions. Because the side polishing process used in D-type sensing probe reduces the mechanical strength of the fiber and takes a long time, whereas microsphere sensing probe increase the mechanical strength of the fiber by making microspheres and are simple to fabricate, different microsphere diameters excite different cladding modes and have different sensing performance. As a result, this article creates probes with varying microsphere dimensions to examine the impacts of resonance band and sensitivity. The diameters of the microspheres were controlled by controlling the number of discharges to be 165 μm, 233 μm, and 306 μm, respectively, to make sensing probes and conduct refractive index sensing experiments, and the refractive indices of the solutions to be measured ranged from 1.333 to 1.385, as shown in Fig. 8.

From the experimental spectrogram in Fig. 8, it can be seen that the SPR resonance valley shifts to long-wavelength direction with the refractive index of the solution to be measured increases, as shown in Figs. 8(a)–8(c). The findings displayed in Fig. 8(d) were obtained by executing a linear fit using the solution refractive index as the horizontal scales and the sensing probe's resonant wavelength as the vertical coordi-

nate. The average sensitivity of the three sizes of microsphere sensing probes was 2288.89 nm/RIU, 2538.01 nm/RIU, and 3182.76 nm/RIU, respectively, with little variation in the dynamic range of their SPR operating wavelengths. We choose the microsphere probe with a diameter of 306 μm to cascade with the D-type probe in this research to create a dual-channel SPR because its SPR resonance valley band varies most from the D-type probes and has the maximum sensitivity.

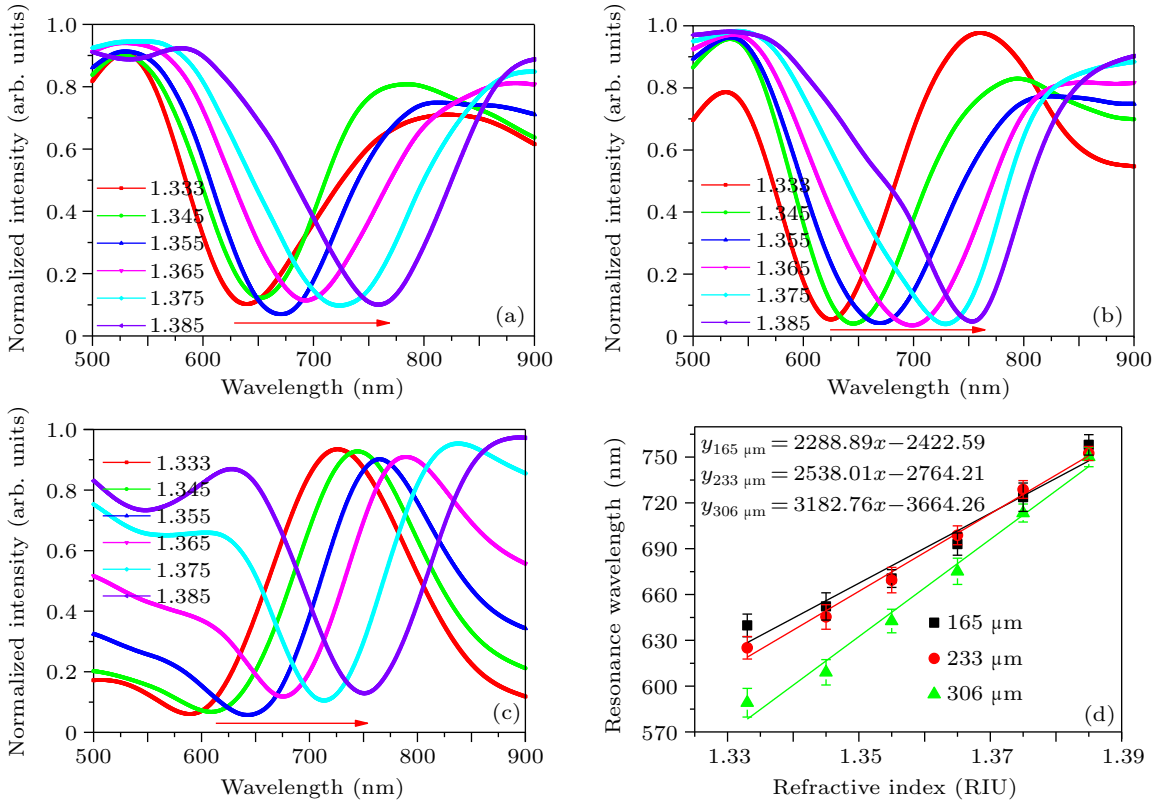



**Fig. 8.** Refractive index test results of SPR probes with different diameter microspheres: (a) 165 μm, (b) 233 μm, (c) 306 μm.

## 4. D-type and microsphere probes cascade testing

Based on the above analysis, the microsphere probe with a diameter of 306 μm is chosen to be cascaded with the D-type probe in this paper, schematic diagram of the dual-channel fiber optic SPR sensing probe is shown in Fig. 9. We positioned the D-type sensing area in the front to form sensing zone A because it requires the ring core mode, and the microsphere sensing area in the back to form the sensing zone B because it needs little requirement for transmission mode. When only the middle core of the coaxial dual waveguide is injected, the transmitted light goes to the middle core, and there is no light in the ring core and side throw area, so the SPR effect does not occur in the sensing zone A. At this time, the transmitted light reaches the microsphere structure to excite the cladding mode, which generates the SPR effect and allows single-channel sensing; when only the ring core of the coaxial dual waveguide is injected, the transmitted light passes through the side throw area and the microsphere structure, and the SPR effect occurs in the sensing zone A and sensing zone B at the same time, which can play a significant role in the field of multi-specimen detection and realize dual-channel SPR detection on one fiber.

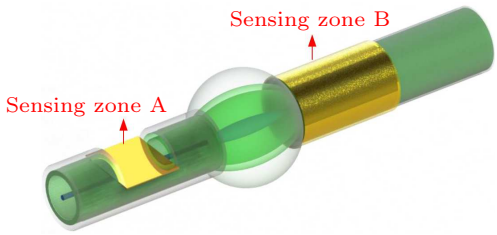



**Fig. 9.** The schematic diagram of the dual-channel fiber optic SPR sensing probe.

Figure 10 depicts a dual-channel refractive index sensing test experimental setup. To clearly separate the resonance valleys of the sensing probe's two sensing zones, we make the thickness of the sensing gold film of sensing zone A 30 nm and the thickness of the sensing gold film of sensing zone B 50 nm; sensing zone A detects low refractive index solutions, and sensing zone B detects high refractive index solutions.

Figure 11 depicts the testing results. Among them, because the spherical sensing stage B is located on the side away from the light source, its resonant light intensity is smaller than that of the D-type sensing region A, as shown in the vignette in Fig. 11. To carry out the comparison of the SPR resonance valley of the two sensing regions, the alignment process of the

resonance valley of the two sensing regions is carried out, and the results are obtained as shown in the large figure in Fig. 11. In Fig. 11(a), the refractive index of the solution to be measured in sensing zone A is 1.333, and the refractive index of the solution to be measured in sensing zone B ranges from 1.375 to 1.405. In Fig. 11(b), the refractive index of the solution to be measured in sensing zone A ranges from 1.333 to 1.365, and the refractive index of the solution to be measured in sensing zone B is fixed at 1.395. In Fig. 11(c), the refractive index of the solution to be measured in sensing zone A ranges from 1.333 to 1.365, and the refractive index of the solution to be measured in sensing zone B ranges from 1.375–1.405.

As shown in Fig. 11, this dual-channel SPR sensor can detect in a single stage, as shown in Figs. 11(a) and 11(b), and it can also sense in two channels simultaneously, as shown in Fig. 11(c). The two-stage SPR resonance valleys in Fig. 11(c) both move toward the long wavelength direction as the external solution's refractive index increases, and the dynamic range of the D-type sensing area A is in the short wavelength range and the dynamic range of the microsphere sensing area B is in the long wavelength range. The dynamic range and detection sensitivity for refractive index were calculated to be 607.4 nm–638.81 nm, 701.96 nm–805.41 nm, and 981.56 nm/RIU, 4138 nm/RIU, respectively.

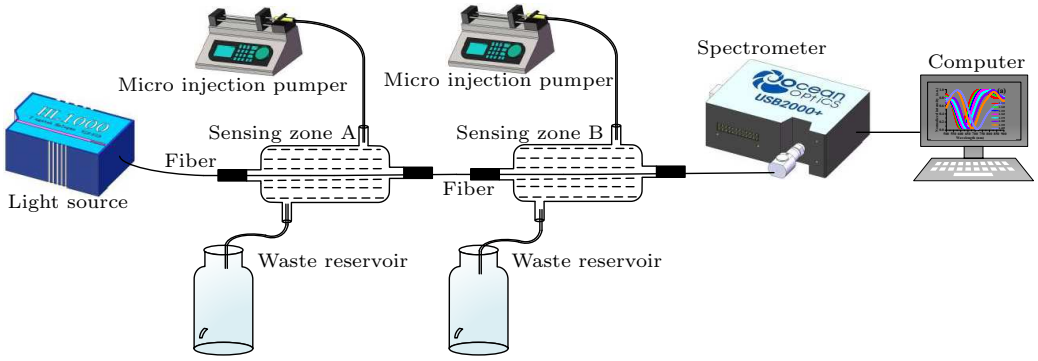



**Fig. 10.** Dual-channel SPR sensor refractive index sensing test experimental setup.

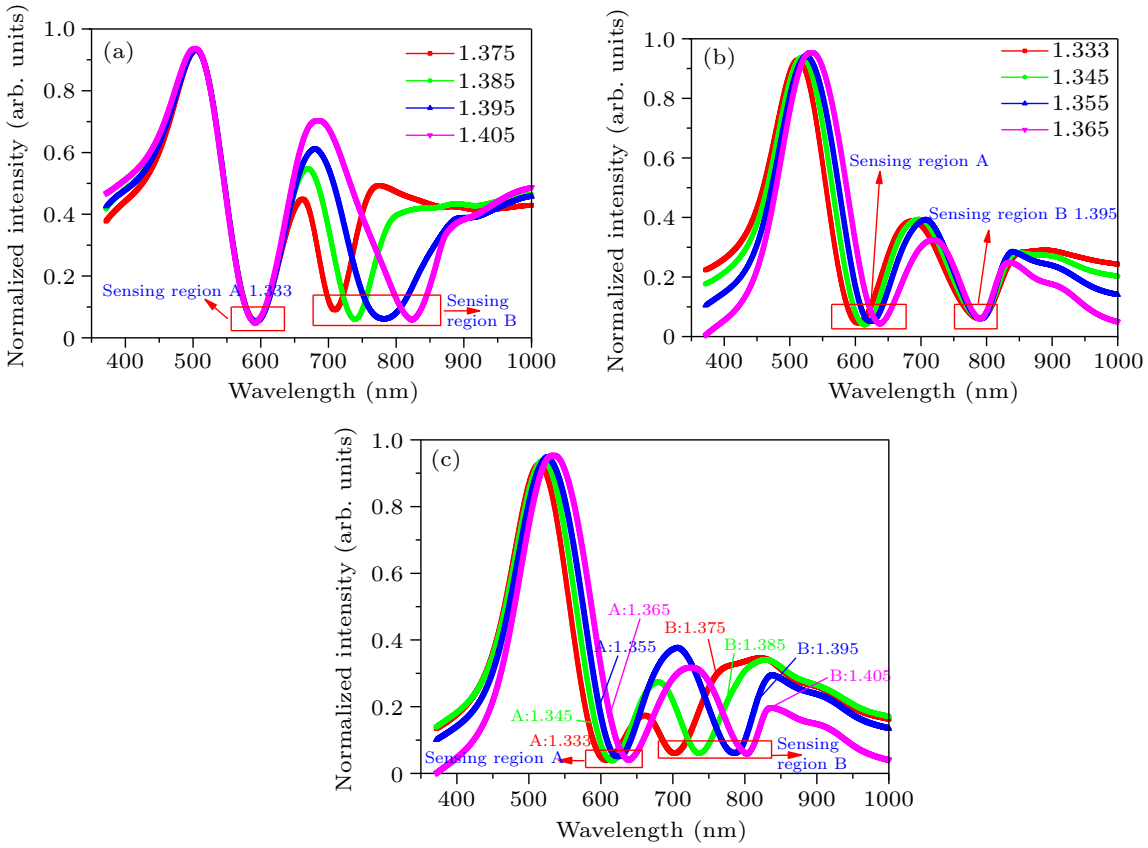



**Fig. 11.** Cascaded dual-channel SPR sensing results and resonance valley alignment data: (a) D-type sensing area A external solution refractive index 1.333, microsphere sensing area B external solution refractive index range 1.375–1.405; (b) D-type sensing area A external solution refractive range 1.333–1.365, microsphere sensing area B external solution refractive index 1.395; (c) D-type sensing area A external solution refractive range 1.333–1.365, microsphere sensing area B external solution refractive index range 1.375–1.405.

**Table 1.** Performances comparison of dual-channel optical-fiber SPR sensors.

| Reference | Channel I | | Channel II | |
|---|---|---|---|---|
| | RI range (RIU) | Sensitivity (nm/RIU) | RI range (RIU) | Sensitivity (nm/RIU) |
| [19] | 1.24–1.3 | 1200 | 1.3–1.36 | 1650 |
| [20] | 1.333–1.385 | 1414 | 1.333–1.385 | 3687 |
| [21] | 1.34–1.36 | 4280 | 1.34–1.36 | 3940 |
| [22] | 1.333–1.385 | 2540.77 | 1.333–1.385 | 2691.57 |
| [23] | 1.333–1.385 | 1980.77 | 1.333–1.385 | 4057.69 |
| This work | 1.333–1.365 | 981.56 | 1.375–1.40 | 4138 |

In addition, compared with other dual-channel optical-fiber SPR sensors, although our sensor with channel I has a lower sensitivity, channel II has a higher sensitivity. What is more, a wide detection range is got (as shown in Table 1). We fabricated dual-channel fiber SPR sensor composed of D-type structure and microspheres, and combined wavelength division multiplexing and space division multiplexing technologies, which provide a novel research idea for multi-channel fiber SPR sensors.

## 5. Conclusion

We propose an optical fiber SPR sensor based on the cascade application of coaxial dual waveguide D-type and spherical structures in this research. The fiber core mode of the ring core of the coaxial dual waveguide provides the evanescent field for the D-type sensing region, and the spherical sensing region provides the evanescent field for the spherical sensing region cladding mode created after the spherical expansion. The refractive index of the spherical sensing zone is optimized for high sensitivity detection by adjusting the radius of the microsphere. Through the cascade test of the two-stage sensing area, its dual-channel sensing capability is proved, and its two-stage refractive index detection sensitivity can reach 981.56 nm/RIU and 4138 nm/RIU, respectively. The dual-channel SPR sensor integrates wavelength division multiplexing and space division multiplexing technology, which solves the problem of difficult separation of multi-level resonance valleys., and is simple to fabricate, stable in structure, and can be widely used in micro-space biochemical sensing after surface modification.

## Acknowledgments

Project supported by the National Natural Science Foundation of China (Grant No. 61705025), the Natural Science Foundation of Chongqing (Grant Nos. cstc2019jcyj-msxmX043 and cstc2018jcyjAX0817), the Fund from the Science and Technology Project Affiliated to the Education Department of Chongqing Municipality (Grant Nos. KJQN201801217, KJQN202001214, KJQN201901226, and KJ1710247), the Fund from Chongqing Key Laboratory of Geological Environment Monitoring and Disaster Early-Warning in Three Gorges Reservoir Area (Grant Nos. ZD2020A0103 and ZD2020A0102), and the Fundamental Research Funds for Chongqing Three Gorges University of China (Grant No. 19ZDPY08).

## References

[1] Peeters B, Daems D, Van der Donck T, Delport F and Lammertyn J 2019 *ACS Appl. Mater.* **11** 6759
[2] Chen Z, Han K and Zhang Y N 2019 *Appl. Sci.* **9** 1480
[3] Narsaiah K, Jha S N, Bhardwaj R, Sharma R and Kumar R 2012 *J. Food Sci.* **49** 383
[4] Kretschmann E and Raether H 1968 *Zeitschrift für Naturforschung A* **23** 2135
[5] Liu Z, Wei Y, Zhang Y, Sun B, Zhao E, Zhang Y, Yang J and Yuan L 2015 *Sensors Actuators B: Chemical* **221** 1330
[6] Liu Z, Wei Y, Zhang Y, Liu C, Zhang Y, Zhao E, Yang J, Liu C and Yuan L 2015 *Opt. Lett.* **40** 4452
[7] Liu Z, Wei Y, Zhang Y, Zhang Y, Zhao E, Yang J and Yuan L 2015 *Opt. Lett.* **40** 2826
[8] Liu C, Zhang X, Gao Y, Wei Y, Wu P, Su Y and Wu P 2020 *Appl. Opt.* **59** 1323
[9] Zhou X, Li S, Li X, Yan X, Zhang X, Wang F and Cheng T 2020 *IEEE Trans. Instrum. Measur.* **69** 8494
[10] Zhang Y, Liang P, Wang Y, Zhang Y, Liu Z, Wei Y, Zhu Z, Zhao E, Yang J and Yuan L 2017 *Sensors Actuators A: Physical* **267** 526
[11] Yu H, Chong Y, Zhang P, Ma J and Li D 2020 *Talanta* **219** 121324
[12] Sun Y S, Li C J and Hsu J C 2016 *Sensors* **17** 63
[13] Singh S, Srivastava A, Pandey S K and Prajapati Y K 2022 *Recent Trends in Electronics and Communication* (Springer) p. 299
[14] Vindas K, Leroy L, Garrigue P, Voci S, Livache T, Arbault S, Sojic N, Buhot A and Engel E 2019 *Analytical Bioanalytical Chemistry* **411** 2249
[15] Coelho L C C, de Almeida J M M M, Moayyed H, Santos J L and Viegas D 2015 *Journal of Lightwave Technology* **33** 432
[16] Korec J, Stasiewicz K A, Jaroszewicz L R and Garbat K 2020 *Materials* **13** 4942
[17] Al-Qazwini Y, Noor A, Yaacob M H, Harun S W and Mahdi M 2015 *Sensors Actuators A: Physical* **236** 38
[18] Wu Z, Shum P P, Shao X, Zhang H, Zhang N, Huang T, Humbert G, Auguste J L, Gérome F and Blondy J M 2016 *Opt. Lett.* **41** 380
[19] Nasirifar R, Danaie M and Dideban A 2019 *Optik* **186** 194
[20] Wang R, Liu C, Wei Y, Jiang T, Liu C, Shi C, Zhao X and Li L 2022 *Optik* **266** 169603
[21] Jiao S, Ren X, Yang H, Xu S and Li X 2022 *Plasmonics* **17** 295
[22] Wei Y, Zhao X, Liu C, Wang R, Jiang T, Li L, Shi C, Liu C and Zhu D 2023 *Chin. Phys. B* **32** 030702
[23] Liu Z, Liu L, Zhu Z, Zhang Y, Wei Y, Zhang Y, Yang J and Yuan L 2017 *Opt. Commun.* **403** 290